Oridonin ameliorates ulcerative colitis by regulating the PI3K/AKT/mTOR signaling pathway to activate autophagy

ZHONGXING MIAO[1,2*], BAOHONG LIU[3*], XINGZHI ZHOU[2*], MENGRU LU[2], NI JIA[2], HUAMIN ZHANG[4], YING QI[2], XIAOYU TAN[5] and QINGGAO ZHANG[1,2]

[1]Immunology Biology Key Laboratory, Yanbian University, Yanji, Jilin 133002, P.R. China; [2]Health Medicine Translational Research Center, School of Basic Medical Sciences, Dalian University, Dalian, Liaoning 116622, P.R. China; [3]Department of Medical Supervision, Tianjin Binhai New Area Center for Disease Control and Prevention, Tianjin 300451, P.R. China; [4]Department of Central Laboratory, Affiliated Zhongshan Hospital of Dalian University, Dalian, Liaoning 116001, P.R. China; [5]Department of Clinical Laboratory, Xin Hua Hospital Affiliated to Dalian University, Dalian, Liaoning 116021, P.R. China

Received December 17, 2025; Accepted April 24, 2026

DOI: 10.3892/ijmm.2026.5894

Abstract. The present study aimed to investigate the therapeutic effects and underlying mechanism of oridonin (ORI) in ulcerative colitis (UC) using the lipopolysaccharide (LPS)-induced macrophage inflammatory model *in vitro* and the dextran sulfate sodium (DSS)-induced mouse UC model *in vivo*. Cell Counting Kit-8 assay was used to determine the appropriate drug concentrations for the *in vitro* experiments. Western blotting and reverse transcription-quantitative polymerase chain reaction were performed to evaluate the expression levels of proteins and mRNAs related to signaling pathways, autophagy and inflammatory cytokines. The autophagy inhibitor 3-methyladenine was applied to verify the role of the PI3K/AKT/mTOR pathway. *In vivo*, the disease activity index (DAI) was recorded and colon tissue damage was assessed by hematoxylin and eosin staining. Serum inflammatory cytokines were measured using an enzyme-linked immunosorbent assay. Network pharmacology based on GeneCards and Traditional Chinese Medicine Systems Pharmacology databases, along with Gene Ontology and Kyoto Encyclopedia of Genes and Genomes enrichment analysis, predicted involvement of the PI3K/AKT/mTOR pathway in the pathogenesis of UC, which was further validated by the immunohistochemistry, immunofluorescence and western blotting of colon tissues. The results indicated that ORI significantly reduced the expression of pro-inflammatory cytokines and increased the anti-inflammatory cytokine interleukin-10 in LPS-stimulated macrophages. In DSS-induced colitis mice, ORI treatment alleviated body weight loss, decreased DAI scores, improved colon shortening and upregulated the expression of intestinal tight junction proteins. Mechanistically, ORI inhibited the PI3K/AKT/mTOR pathway and altered autophagy-related molecular markers, as evidenced by increased levels of autophagy-related (ATG)13, beclin-1, ATG12, ATG7 and ATG5 as well as decreased expression of p62. In conclusion, ORI alleviates inflammatory responses *in vitro* and mitigates UC-related pathological changes *in vivo*, which may be associated with suppression of the PI3K/AKT/mTOR pathway and modulation of autophagy-associated protein markers.

Correspondence to: Professor Qinggao Zhang, Immunology Biology Key Laboratory, Yanbian University, 977 Gongyuan Road, Yanji, Jilin 133002, P.R. China
E-mail: zhangqinggao@dlu.edu.cn

Mrs. Xiaoyu Tan, Department of Clinical Laboratory, Xin Hua Hospital Affiliated to Dalian University, 156 Wansui Street, Dalian, Liaoning 116021, P.R. China
E-mail: 171263371@qq.com

*Contributed equally

Key words: ulcerative colitis, oridonin, PI3K/AKT/mTOR, autophagy, inflammation

Introduction

Ulcerative colitis (UC), a type of inflammatory bowel disease (IBD), is characterized by chronic, relapsing, non-specific inflammation; its core pathological mechanisms involve disruption of intestinal immune homeostasis and compromise of the mucosal barrier (1). Clinically, UC is distinguished from Crohn's disease primarily by anatomical involvement. Although both disorders share symptoms such as abdominal pain, diarrhea, rectal bleeding and bloody mucopurulent stools, UC is typically confined to the colonic mucosa, causing inflammation and ulceration of the superficial intestinal layers. By contrast, Crohn's disease can affect any part of the gastrointestinal tract and features deeper transmural ulcers (2). In 2023, there were ~5 million cases of UC globally, with the highest incidence in Northern Europe, North America and Oceania. In Asia, prevalence is projected to increase up to four-fold by 2035 (3).

Current UC management strategies include pharmacological and non-pharmacological approaches. Pharmacological treatments encompass 5-aminosalicylic acid

(5-ASA), corticosteroids, immunosuppressants and biologics. Non-pharmacological options include newer methods such as leukocytapheresis, fecal microbiota transplantation and nutritional therapy (4). However, conventional drugs often produce unsatisfactory outcomes, with patients developing resistance and experiencing adverse effects such as intestinal dysbiosis, which substantially diminish their quality of life. While emerging therapies are innovative and practicable, their high costs impose a considerable economic burden on patients (5).

The PI3K/AKT/mTOR signaling pathway regulates various physiological processes, including cell metabolism, growth and survival (6). Aberrant activation of this pathway is well-documented in patients with UC and experimental models, where hyperactivation promotes transcription and secretion of pro-inflammatory cytokines, such as interleukin (IL)-6, IL-1β and tumor necrosis factor-α (TNF-α), triggering a robust inflammatory cascade (7). These cytokines recruit and activate immune cells, disrupting the intestinal mucosal barrier and amplifying the inflammatory cascade, thereby exacerbating UC symptoms (8). Given the pivotal role of this pathway in inflammation, targeting the inhibition of PI3K/AKT/mTOR is a potential therapeutic strategy for UC, as demonstrated by rhein effectively mitigating experimental colitis by inhibiting the PI3K/AKT/mTOR signaling pathway (7). The PI3K/AKT/mTOR pathway does not operate in isolation; rather, it exhibits extensive crosstalk with key inflammatory pathways such as NF-κB and MAPK. Activation of the pathway can indirectly enhance the transcriptional activity of NF-κB by phosphorylating downstream targets, forming positive feedback loops that collectively upregulate the expression of pro-inflammatory mediators (8). These networked interactions establish the PI3K/AKT/mTOR pathway as a critical hub connecting cellular metabolism, survival signals and inflammatory responses, rendering its role in UC even more complex and significant. Notably, mTORC1 serves as a key negative regulator of autophagy, primarily by suppressing the expression of various autophagy-related (ATG) proteins and impacting the autophagic process (9). Building on these insights and supported by network pharmacology predictions, the present study focused on the PI3K/AKT/mTOR signaling pathway as a central mechanistic avenue.

Autophagy disruption is another critical factor in UC pathogenesis. Macroautophagy and microautophagy are highly conserved processes in eukaryotic cells involving the lysosomal degradation of cytoplasmic materials, regulated by gene products such as ATG proteins (10). During inflammation, autophagosome formation begins with activation of unc-51 like autophagy activating kinase 1 (ULK1), which forms a complex with proteins such as ATG13 and FIP200. Upon initiation of the ULK1 complex, involvement of the ATG12-ATG5-ATG16L system and ATG7 catalyzes the conjugation of LC3 to phosphatidylethanolamine, facilitating conversion from LC3-I to LC3-II. Following autophagosome formation, fusion with the lysosome forms an autolysosome for the degradation of its contents (11). In UC, persistent inflammation inhibits the activation and effector roles of ATG proteins and the surge in inflammatory factors can silence ATG gene expression (12). Research indicates that suppressed autophagy can activate NF-κB, leading to the release of pro-inflammatory cytokines. For example, ATG5 deficiency elevates reactive oxygen species (ROS) levels, while ATG7 deficiency triggers inflammasome activation, reduces intestinal occludin levels and increases epithelial permeability, thereby influencing UC progression (13). Thus, we propose that using natural Chinese medicine to enhance colonic autophagy could help clear inflammatory cytokines, protect the mucosal barrier and alleviate UC symptoms.

In recent years, Chinese herbal medicine has attracted widespread academic interest in medical research for its multi-target effects, minimal side effects and reduced recurrence rates (14). Oridonin (ORI), a natural terpenoid compound from the Chinese herb *Rabdosia rubescens* (15), exhibits a broad spectrum of pharmacological activities, including anticancer, anti-inflammatory and protective effects on the liver, kidneys and heart (16). Specifically, ORI inhibits the NF-κB pathway to mitigate inflammation in osteoarthritis (17). Evidence suggests that ORI exerts anti-breast cancer activity by suppressing the PI3K/AKT pathway (18). Moreover, ORI has been reported to boost autophagic flux and accelerate autophagosome formation, thereby contributing to its anti-inflammatory role in autoimmune diseases (19). ORI has also shown efficacy in relieving symptoms associated with colon cancer (20). Given these properties, ORI was selected as the investigational compound for UC treatment in the present study.

The present study aimed to investigate the inhibitory effect of ORI on inflammation *in vitro*, confirm its efficacy in alleviating UC symptoms in model mice and utilize network pharmacology along with validation experiments to elucidate the potential mechanism through which ORI exerts its anti-inflammatory effects and mitigates UC symptoms. The findings are intended to provide new experimental evidence for the treatment of UC and the further development and clinical application of ORI.

Materials and methods

Reagents. ORI (high-performance liquid chromatography purified, ≥98%; cat. no. WKQ-0000182) was purchased from Sichuan Weikeqi Biotechnology Co., Ltd. Lipopolysaccharide (LPS), 5-ASA and carboxymethyl cellulose sodium (CMC-Na) were obtained from MilliporeSigma. 3-Methyladenine (3-MA) was procured from AbMole Bioscience. ATP was provided by Coolaber Science & Technology. Dextran sulfate sodium (DSS) was purchased from MP Biomedicals, LLC. Dulbecco's Modified Eagle Medium (DMEM) was obtained from Gibco (Thermo Fisher Scientific, Inc.). A Cell Counting Kit-8 (CCK-8) assay kit was acquired from APeXBIO Technology LLC. The total protein extraction kit and TriQuick Reagent for RNA extraction were supplied by Beijing Solarbio Science & Technology Co., Ltd. A specific reverse transcription (RT) kit for RT-polymerase chain reaction (RT-PCR) and TB Green® Premix Ex Taq™ II were purchased from Takara Biotechnology Co., Ltd.

Cell culture. RAW264.7 mouse macrophages, purchased from the American Type Culture Collection (ATCC), were cultured in DMEM supplemented with 10% fetal bovine serum (Biological Industries; Sartorius AG) and 1% penicillin-streptomycin (Gibco; Thermo Fisher Scientific, Inc.). The cells were

cultured in a 5.0% CO_2 atmosphere at 37˚C. THP-1 human acute monocytic leukemia cells, also obtained from ATCC, were maintained in RPMI-1640 medium containing 10% fetal bovine serum and 1% penicillin-streptomycin. Both cell lines were used for *in vitro* assays.

Network pharmacology databases. The GeneCards database (http://www.genecards.org) was used to retrieve disease-related genes, the STRING database (https://www.string-db.org/) was employed for protein-protein interaction (PPI) analysis and the DAVID database (https://david.ncifcrf.gov/) was utilized for Gene Ontology (GO) enrichment analysis and Kyoto Encyclopedia of Genes and Genomes (KEGG) pathway enrichment analysis. Cytoscape software (v3.9.1; https://cytoscape.org/download.html) was used to visualize target-pathway networks. The chemical structure of ORI was retrieved and confirmed using the PubChem database (https://pubchem.ncbi.nlm.nih.gov/). Potential target proteins of ORI were systematically collected from two publicly accessible online databases: The Traditional Chinese Medicine Systems Pharmacology (TCMSP) database (http://old.tcmsp-e.com/tcmsp.php) and the Bioinformatics Analysis Tool for Molecular Mechanisms of Traditional Chinese Medicine (BATMAN-TCM) database (http://bionet.ncpsb.org.cn/batman-tcm/).

CCK-8 cell viability assay. Cells in good growth condition, with regular morphology, clear cell margins and no overcrowding, were collected and seeded into 96-well plates at 100 μl per well (100,000 cells/ml). After overnight incubation at 37˚C with 5% CO_2, cells were treated with various concentrations of ORI for 24 h. Then, 10 μl of CCK-8 solution was added to each well and incubated at 37˚C for 4 h in the dark. The optical density (OD) was measured at 450 nm.

Cellular inflammation model. RAW264.7 and THP-1 cells were randomly divided into five groups: Control, LPS, ORI high-dose (ORI-H; 20 μM), LPS + ORI low-dose (ORI-L; 10 μM) and LPS + ORI-H. After removing the old medium, fresh medium with or without ORI was added accordingly. ORI-treated groups were incubated with the corresponding concentrations of ORI at 37˚C for 18 h. After this, the LPS and LPS + ORI groups were stimulated with 1 μg/ml LPS at 37˚C for 6 h. Cells were then collected for subsequent experiments.

Animal model. Wild-type C57BL/6 male mice, 6-8 weeks old and weighing 18-22 g, were purchased from Shenyang Changsheng Biotechnology Co., Ltd. Before the experiment, all mice were acclimatized for 1 week under standard housing conditions (22±2˚C, humidity 55-65%, light period from 6:00 to 18:00 and ambient pressure) with free access to food and water. All animal procedures were conducted in compliance with the Guide for the Care and Use of Laboratory Animals. This study combined with the pathological characteristics of DSS-induced UC model mice, formulated quantifiable humane endpoint criteria, including weight loss ≥20% compared with the baseline, persistent unrelieved severe UC-related symptoms, abnormal motor and mental status and abnormal signs and complications. Euthanasia was performed immediately if any one of the criteria appeared and persisted for >24 h. During the experiment, the body weight of the model mice was recorded regularly every day. In the DSS model group, 3 mice showed a body weight loss of >20% on the 7th day, euthanasia was performed humanely by intravenous injection of an excessive dose of sodium pentobarbital (200 mg/kg).

A total of 30 male C57BL/6 mice were divided into five groups (n=6 per group): Control, DSS, DSS + 5-ASA (200 mg/kg), DSS + ORI-L (6 mg/kg) and DSS + ORI-H (12 mg/kg). Mice in the ORI treatment groups received daily oral gavage of ORI dissolved in 5% CMC-Na for 14 days. The positive control group (DSS + 5-ASA) received 200 mg/kg 5-ASA in 5% CMC-Na via daily oral gavage. The control and DSS groups received 5% CMC-Na daily. Starting from day 8, all groups except the control were given 3% DSS in drinking water for 7 days to induce acute UC. Body weight, mental status, fecal characteristics and bleeding were recorded daily. The experiment was repeated at least three times. Following the final observations, blood samples were collected via the orbital venous plexus (0.5-1.0 ml of blood from each mouse) under general anesthesia (intraperitoneal injection of sodium pentobarbital at a dose of 50 mg/kg). Mice were euthanized by cervical dislocation immediately after blood collection. Colon tissues were rapidly excised, measured and sampled for further analysis. The Disease Activity Index (DAI) was calculated based on weight loss, stool consistency and bleeding, using the formula: DAI=(weight loss index + stool consistency score + bleeding score)/3.

Hematoxylin and eosin (H&E) staining. Fresh colon tissues were fixed in 4% paraformaldehyde at 4˚C for >24 h. After routine processing, paraffin-embedded sections were cut at 2-4 μm thickness and stained with H&E (hematoxylin for 8 min and eosin for 1 min at room temperature) for histological evaluation, including damage and ulceration of the colon epithelium, vascular congestion and erosion as well as necrosis of intestinal mucosal epithelial cells under an optical microscope (Olympus Corporation).

Western blotting. The colon tissue samples (~0.1 g per sample) were collected from three randomly selected mice in each experimental group and homogenized in radioimmunoprecipitation assay (RIPA) lysis buffer for protein extraction. For cultured cells, following treatment, adherent cells were detached using pre-chilled phosphate-buffered saline and collected via centrifugation at 600 x g for 5 min at 4˚C. After supernatant removal, the cell pellet was resuspended in RIPA buffer for lysis. The protein concentration was accurately quantified via the BCA assay (Beijing Solarbio Science & Technology Co., Ltd.) and denatured samples were prepared for electrophoresis. Each electrophoresis lane was loaded with 20 μg of total protein. The proteins were separated by 6-15% SDS-PAGE and transferred onto PVDF membranes (MilliporeSigma). The membranes were blocked with 5% non-fat milk (20 ml) for 1 h at room temperature, followed by overnight incubation with primary antibodies at 4˚C. Subsequently, the membranes were washed three times with PBST (PBS containing 0.1% Tween-20) and incubated with appropriate HRP-conjugated secondary antibodies for 1 h at room temperature. Finally, protein bands were visualized using the cECL Western Blot Kit (CWBio; Jiangsu Kangwei Century Biotechnology Co., Ltd.). Blots were visualized using

a chemiluminescence imaging system (Chemi Dog Ultra; Shanghai Tanon Science & Technology Co., Ltd.). Band intensities were analyzed with ImageJ software (National Institutes of Health). Detailed antibody specifications and supplier information are outlined in Table SI.

RT-quantitative PCR (RT-qPCR). RNA was extracted using TriQuick Reagent. Genomic DNA was removed in a reaction containing 2 μl RNA (1 μg), 2 μl 5X gDNA Eraser Buffer, 1 μl gDNA Eraser and 5 μl RNase-free dH_2O. The cDNA was synthesized using the PrimeScript™ RT reagent Kit with gDNA Eraser (Takara Bio, Inc.) following the manufacturer's instructions, with the specific temperature protocol as below: RNA denaturation at 65˚C for 5 min, followed by immediate placement on ice for 2 min to prevent RNA renaturation; RT at 37˚C for 15 min; enzyme inactivation at 85˚C for 5 sec to terminate the reaction. The synthesized cDNA was stored at -20˚C for subsequent qPCR experiments.

qPCR was conducted on a StepOnePlus™ Real-Time PCR System (Applied Biosystems; Thermo Fisher Scientific, Inc.) using the SYBR® Premix Ex Taq™ II Kit (Takara Bio, Inc.). The thermocycler conditions were set as follows: Pre-denaturation at 95˚C for 30 sec; amplification cycle (40 cycles) at 95˚C for 5 sec and 60˚C for 30 sec; melting curve analysis at 95˚C for 15 sec, 60˚C for 1 min and then heating to 95˚C at a rate of 0.3˚C per sec. Glyceraldehyde-3-phosphate dehydrogenase was selected as the internal reference gene in this study. The relative expression level of the target gene was quantified using the $2^{-\Delta\Delta Cq}$ method (21). Primer sequences are provided in Table SII.

Enzyme-linked immunosorbent assay (ELISA). Blood was collected from the mouse orbital venous plexus and centrifuged at 900 x g at room temperature for 10 min to isolate the supernatant serum. The captured antibodies against mouse IL-6, TNF-α, IL-10 and IL-1β (Table SI) were pre-coated onto microwells. The OD of each well was measured at 450 nm and the cytokine concentrations were determined based on the standard curve.

Immunohistochemistry (IHC). IHC was performed to determine the expression levels of IL-6, TNF-α, IL-10 and IL-1β in colon tissues from the DSS, 5-ASA and ORI treatment groups. Tissues were fixed in 4% paraformaldehyde at 4˚C for 24 h, embedded in paraffin and sectioned at 4-6 μm. Antigen retrieval was performed using 3% citrate buffer at 98˚C for 20 min. Endogenous peroxidase activity was quenched with 3% H_2O_2 for 10 min at room temperature. Non-specific binding was blocked with 5% non-fat milk for 60 min at room temperature. Permeabilization was performed with 0.1% Triton X-100 for 15 min. Sections were incubated overnight at 4˚C with the primary antibodies listed in Table SI. This was followed by incubation with HRP-conjugated secondary antibody (Table SI) for 1 h at room temperature. Detection was performed using DAB chromogen (2-step plus Poly-HRP Anti Rabbit/Mouse IgG Detection System; Elabscience Bionovation Inc.) and slides were counterstained with hematoxylin. The sections were observed and imaged under a light microscope (Olympus Corporation). The mean OD was analyzed using ImageJ software. A higher mean density value indicated stronger protein expression, while a lower value suggested weaker expression.

Immunofluorescence assay. Immunofluorescence staining was conducted using the beclin antibody to evaluate autophagy activation in colon tissues across different experimental groups. Additionally, the mTOR antibody was used to assess the status of the PI3K/AKT/mTOR pathway. Fresh tissue specimens were immersed in 4% paraformaldehyde solution for 24 h at 4˚C and cut into 4-6 μm sections. Tissue antigen retrieval was conducted in 3% citrate buffer under continuous heating at 95-98˚C for 20 min. After thermal repair, slices were gradually rehydrated through a series of gradient ethanol solutions (100, 95, 80 and 70%, 2 min each) and washed three times with PBS, each lasting 5 min. To facilitate the labeling of intracellular targets, tissue slices were treated with 0.1% Triton X-100 for 15 min under ambient conditions. Background interference was minimized by sealed incubation with 5% non-fat milk containing 0.1% Tween-20 for 1 h at room temperature. Afterwards, tissue slices were cultured with the following primary antibodies at 4˚C overnight: Anti-F4/80 (cat. no. GB11027; 1:500; Wuhan Servicebio Technology Co., Ltd.), beclin (cat. no. A22361; 1:100; ABclonal Biotech Co., Ltd.) and phospho-mTOR (Ser2448) (cat. no. AF3308; 1:100; Affinity Biosciences). After primary antibody incubation, fluorescent secondary antibodies (cat. no. S0018; 1:100; Affinity Biosciences) were added for a 60-min light-shielded incubation at room temperature. Cell nuclei were dyed with 1 μg/ml DAPI working solution at room temperature for 5 min, then all slices were sealed with anti-fading mounting medium. High-resolution tissue imaging was observed with a fluorescence microscope (Olympus Corporation). ImageJ software was employed for quantitative analysis of the immunofluorescence results.

Statistical analysis. All experiments were independently repeated at least three times. Data are presented as mean ± standard deviation. Statistical analyses were performed using GraphPad Prism version 10.1.2 (Dotmatics). Differences between two groups were analyzed using the unpaired Student's t-test, while comparisons among three or more groups were evaluated by one-way analysis of variance followed by Tukey's HSD post hoc test. $P<0.05$ was considered to indicate a statistically significant difference.

Results

Anti-inflammatory effects of ORI in vitro. To evaluate the anti-inflammatory effects of ORI *in vitro*, the cytotoxic effects of ORI were first assessed using the CCK-8 assay (22). When the ORI concentration reached 64 μM, cell viability decreased to below 50% (Fig. 1A). The LPS-stimulated RAW264.7 cells were treated with different doses of ORI. RT-qPCR results indicated that 10 μM ORI significantly inhibited IL-6 and moderately promoted IL-10 expression (Fig. 1B).

To further investigate the effect of ORI in RAW264.7 cells, key inflammatory cytokines were detected using ELISA, western blot and RT-qPCR (23). Treatment with ORI-H alone did not affect cytokine expression, showing no statistical difference compared with the control group. LPS stimulation

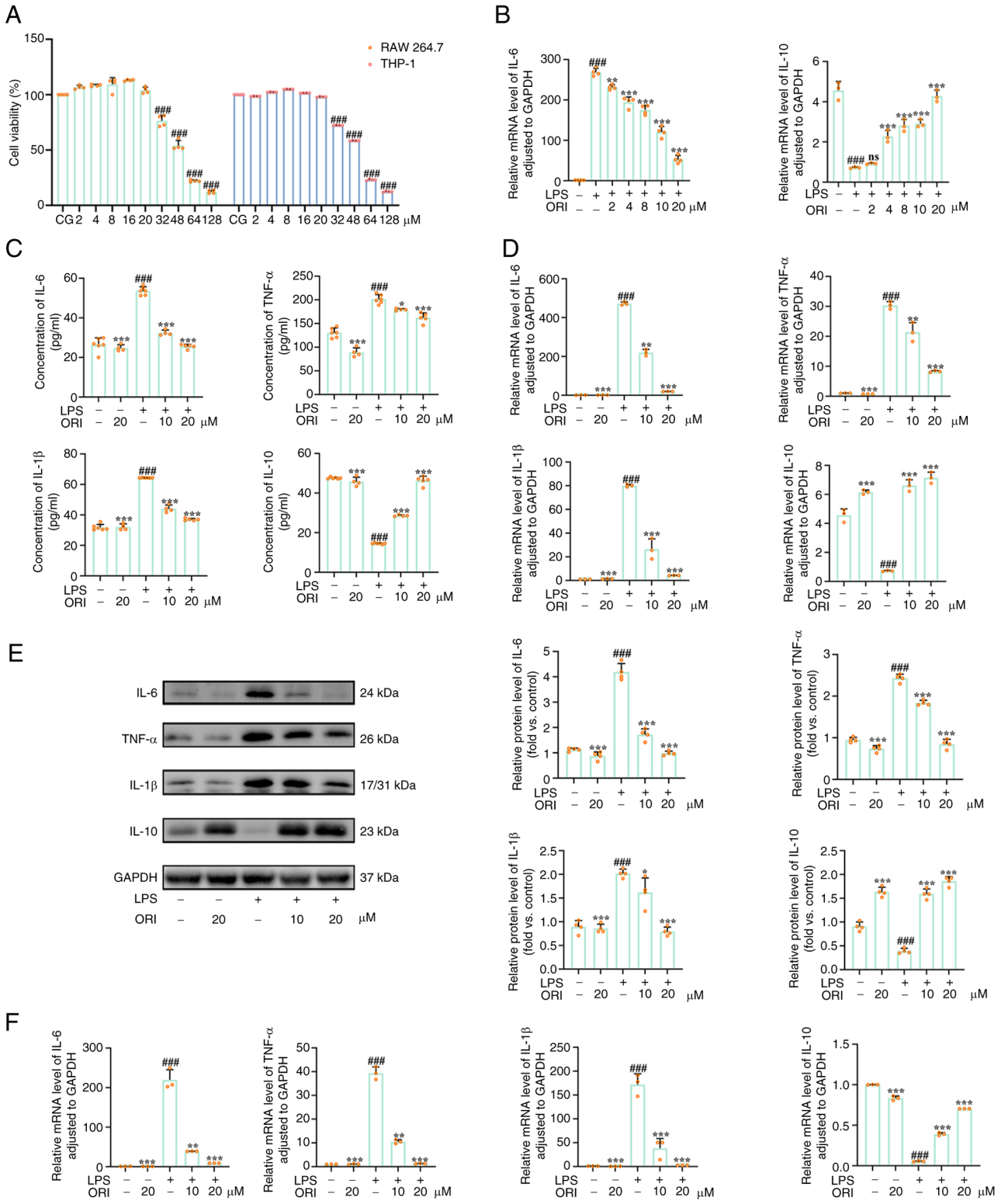

Figure 1. ORI cytotoxicity and its effects on inflammatory factors were evaluated. (A) Cell Counting Kit-8 was used to detect the toxic effects of ORI. (B) The effects of different concentrations of ORI solution on the expression levels of IL-6 and IL-10. (C) Enzyme-linked immunosorbent assay for the secretion of IL-6, TNF-α, IL-1β and IL-10 in the supernatants of cells treated with LPS. (D) RT-qPCR was employed to determine the mRNA contents in cells. (E) Western blot detected the protein level in cells. (F) RT-qPCR was employed to determine the mRNA contents in cells. Comparison with the control group: $^{\#\#}$P<0.01, $^{\#\#\#}$P<0.001; comparison with the LPS group: **P<0.01, ***P<0.001. ORI, oridonin; CG, control group; LPS, lipopolysaccharide; RT-qPCR, reverse transcription-quantitative polymerase chain reaction; IL, interleukin; GAPDH, glyceraldehyde-3-phosphate dehydrogenase; TNF, tumor necrosis factor.

markedly increased the levels of pro-inflammatory cytokines and suppressed the anti-inflammatory cytokine IL-10. ORI treatment notably reversed these LPS-induced alterations, with the LPS + ORI-H group exhibiting results closer to the control group than the LPS + ORI-L group (Fig. 1C). Both RT-qPCR (Fig. 1D) and western blot (Fig. 1E) analyses further confirmed that ORI suppressed the pro-inflammatory cytokine expression and enhanced the release of anti-inflammatory cytokines.

These observations support an association between ORI exposure and attenuated inflammatory responses in RAW264.7 cells *in vitro*. To determine whether the anti-inflammatory effect of ORI is cell-specific, THP-1 cells were treated with ORI and subjected to RT-qPCR analysis of inflammatory cytokines. The trend was similar to that observed in RAW264.7 cells (Fig. 1F). Hence, ORI at various concentrations exhibited anti-inflammatory activity *in vitro* and this effect was not cell-specific.

Attenuation of UC symptoms by ORI in vivo. UC-related symptoms and the effects of ORI were evaluated by comparing changes in body weight, DAI scores and colon length. Pretreatment with ORI resulted in body weight trends similar to those of the control group. Starting from day 8, compared with the control group, mice treated with DSS exhibited varying degrees of weight loss. However, administration of 5-ASA, DSS + ORI-L or DSS + ORI-H significantly alleviated DSS-induced weight loss (Fig. 2A). The DSS group showed rapid weight loss and a sharp increase in DAI scores, whereas the 5-ASA, ORI-L and ORI-H groups displayed lower and more gradually increasing DAI scores (Fig. 2A). The DSS group showed obvious bleeding points with colon shortening by 43% compared with the control group. By contrast, treatment with 5-ASA or different doses of ORI effectively reversed DSS-induced colon shortening, yielding results closer to those of the control group (Fig. 2B). These findings demonstrated that ORI administration notably alleviated UC symptoms induced by DSS.

To further investigate whether ORI attenuates DSS-induced colon damage, H&E staining and histopathological evaluation were conducted. The assessment covered characteristic pathological changes, including mucosal damage, necrosis, crypt architecture loss, edema and infiltration of neutrophils and monocytes in submucosal regions (24). H&E results showed that ORI treatment effectively ameliorated pathological colon damage. Compared with the control group, the DSS group exhibited hyperemia, edema, loss of crypts and depletion of intestinal epithelial and goblet cells. By contrast, the DSS + 5-ASA, DSS + ORI-L and DSS + ORI-H groups showed notable improvement in colon histopathology (Fig. 2C). The distribution of $F4/80^+$ macrophages was assessed using immunofluorescence (25). Pronounced macrophage aggregation was observed in the DSS group, which was markedly reduced in the DSS + 5-ASA and DSS + ORI groups, indicating that ORI mitigated DSS-induced macrophage infiltration (Fig. 2D). This observation indicated that ORI mitigated DSS-induced colonic macrophage infiltration but did not confirm phenotypic polarization of macrophages toward an anti-inflammatory profile.

Based on these findings, we hypothesized that the improvement in the colon histological improvements by ORI might be mediated through the regulation of tight junction proteins. Western blot analysis was used to detect the expression levels of ZO-1, occludin and claudin-1. Protein expression was significantly reduced in the DSS group compared with the control group. By contrast, the DSS + 5-ASA, DSS + ORI-L and DSS + ORI-H groups showed markedly increased expression of ZO-1, occludin and claudin-1 compared with the DSS group (Fig. 2E). These data indicated that ORI may be associated with the upregulated expression of tight junction proteins at the molecular level.

Protective effect of ORI against DSS-induced colitis in mice. To localize the inflammatory cytokine expression levels in mouse intestinal cells, IHC was used to perform chromogen labeling of cytokines (including IL-6, TNF-α, IL-1β and IL-10) in the colon (26) and their distribution in intestinal epithelial cells was observed under a microscope. Compared with the control group, pro-inflammatory cytokines were more concentrated in the DSS group, while the intracellular content of the anti-inflammatory cytokine IL-10 was notably low. However, DSS + 5-ASA, DSS + ORI-L and DSS + ORI-H treatment significantly reversed the intracellular distribution of inflammatory cytokines (Fig. 3A).

Meanwhile, an ELISA was conducted on mouse serum. The experimental results demonstrated that the secretion levels of inflammatory cytokines in the DSS group were significantly higher than those in the control group, while the secretion level of IL-10 was significantly lower. Administration of 5-ASA or ORI significantly reduced the expression levels of pro-inflammatory cytokines and increased the secretion level of IL-10 (Fig. 3B). To further verify the effect of ORI, western blot analysis was performed to detect the protein expression levels of inflammation-related cytokines in the colonic tissues (27). Compared with the control group, the expression level of IL-10 in the DSS-treated group was significantly decreased, while the expression levels of IL-6, TNF-α and IL-1β were significantly increased. After treatment with 5-ASA or ORI, the expressions of IL-6, TNF-α and IL-1β were significantly inhibited, while the expression of IL-10 was restored to a certain extent (Fig. 3C). These results confirmed that ORI reduced intestinal inflammatory responses in DSS-induced colitis but did not define the specific macrophage phenotypes responsible for these cytokine changes.

Identifying targets and pathways of ORI in UC through network pharmacology. Based on the prior experiments, network pharmacology was employed to elucidate the targets of action. First, the structure of ORI was determined using the PubChem database (Fig. 4A) (28). Potential target proteins of ORI were retrieved from the TCMSP and BATMAN-TCM databases (29). Topological comparison with UC-related protein targets collected from the GeneCards database identified 54 core overlapping targets (Jaccard similarity coefficient=0.143; Fig. 4B). A PPI network was constructed using the STRING database and visualized with Cytoscape software (30). Among the identified 54 overlapping proteins, IL-6, TNF-α, IL-1β, SRC, NF-κB and BCL2 were closely associated with UC treatment, and PI3K, AKT and mTOR proteins showed strong relevance (Fig. 4B).

To further analyze the interactions and biological functions among these 54 overlapping proteins, the DAVID database was utilized for GO analysis of the potential target genes. The genes were analyzed from three aspects (cellular component, molecular function and biological process) with the top 10 significantly enriched functions in each category being retained for further analysis (31) (Fig. 4C). Concurrently, the KEGG database was used to analyze the highly correlated signaling pathways among the potential genes involved in ORI treatment

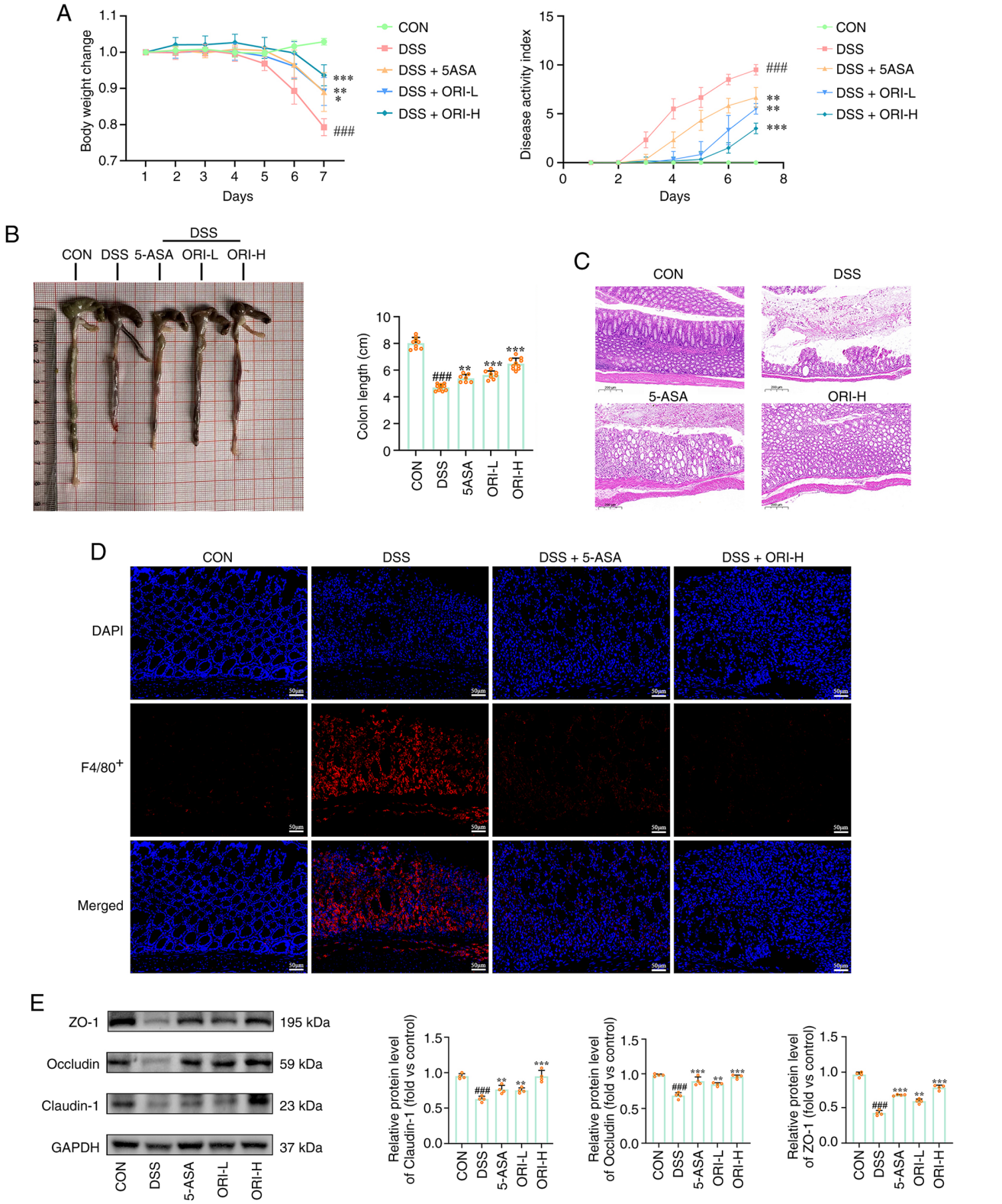

Figure 2. *In vivo* assessment of disease activity, colon morphology, inflammation and tight junction protein expression. (A) Weight change of mice and the Disease Activity Index score. (B) Colonic length image and statistical chart. (C) Hematoxylin and eosin staining of colonic tissues (magnification, x20). (D) Immunofluorescence for the expression of F4/80$^+$ receptor in colonic tissues. (E) Western blot analysis of protein expression of occludin, claudin-1 and ZO-1 in mouse colon tissues. Comparison with the control group: $^{\#\#\#}$P<0.001; comparison with the DSS group: *P<0.05, **P<0.01, ***P<0.001. CON, control; DSS, dextran sulfate sodium; 5ASA, 5-aminosalicylic acid; ORI-L, oridonin low-dose; ORI-H, oridonin high-dose; ZO-1, zonula occludens-1; GAPDH, glyceraldehyde-3-phosphate dehydrogenase.

of UC. The top 20 enriched signaling pathways retained from the enrichment results included the PI3K/AKT/mTOR signaling pathway, which was consistent with the PPI network findings regarding overlapping proteins (Fig. 4C). Therefore, the PI3K/AKT/mTOR signaling pathway may represent a plausible pathway through which ORI exerts its therapeutic effects on UC.

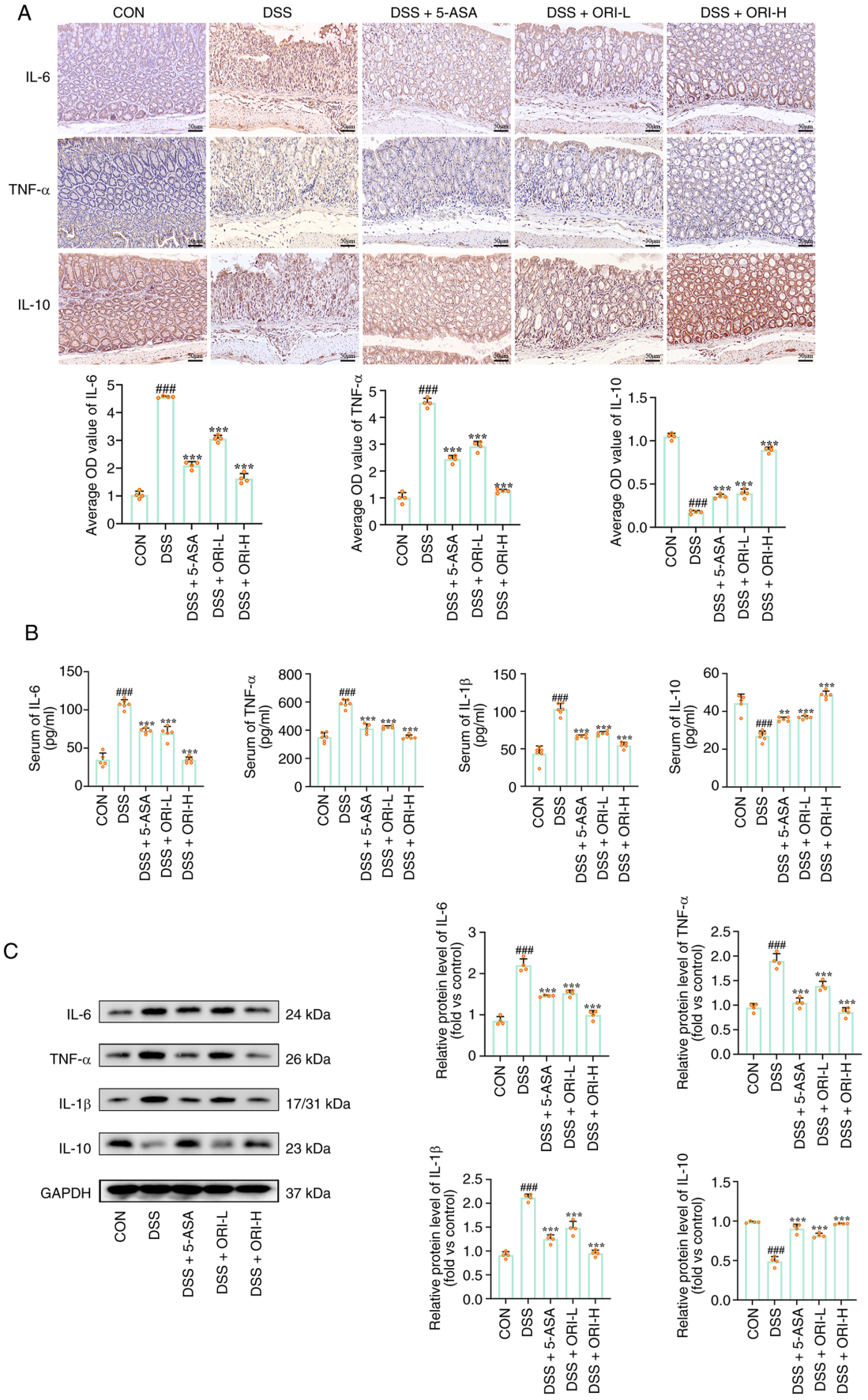

Figure 3. Multi-method evaluation of cytokine expression and secretion in serum and colon tissues. (A) Immunohistochemical staining for IL-6, TNF-α and IL-10 in colonic tissues (magnification, x20) with the mean OD values plotted. (B) Enzyme-linked immunosorbent assay for the secretion in mouse serum. (C) Western blot detection of the protein expression in colon tissues treated with DSS. Comparison with the control group: $^{###}$P<0.001; comparison with the DSS group: **P<0.01, ***P<0.001. CON, control; DSS, dextran sulfate sodium; 5ASA, 5-aminosalicylic acid; ORI-L, oridonin low-dose; ORI-H, oridonin high-dose; OD, optical density; IL, interleukin; TNF, tumor necrosis factor; GAPDH, glyceraldehyde-3-phosphate dehydrogenase.

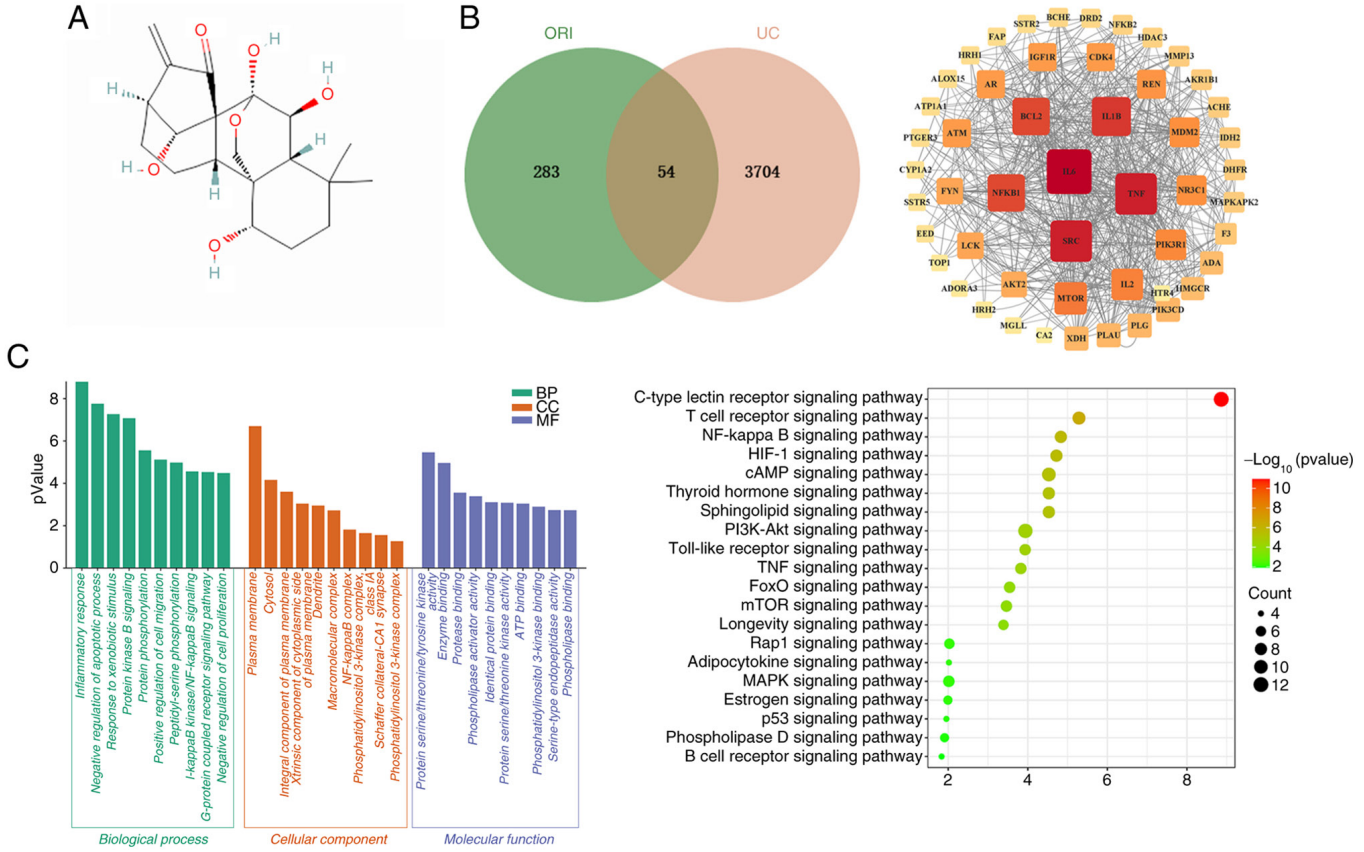

Figure 4. Network pharmacology analysis of ORI-associated proteins for treating UC. (A) The structure of ORI as predicted by the PubChem database. (B) Venn diagram for the overlapping proteins between UC-related and ORI-related target genes and protein-protein interaction network of overlapping target genes. (C) Gene Ontology and Kyoto Encyclopedia of Genes and Genomes analysis of the predicted proteins of ORI for the UC treatment. ORI, oridonin; UC, ulcerative colitis; BP, Biological Process; CC, Cellular Component; MF, Molecular Function.

ORI is associated with suppressed activation of the PI3K/AKT/mTOR signaling pathway. The PI3K/AKT/mTOR signaling pathway is closely associated with critical biological processes such as inflammation and apoptosis, and its aberrant activation is a hallmark feature in patients with UC, indicating its significant role in UC pathogenesis (32). To investigate whether ORI is associated with changes in the PI3K/AKT/mTOR pathway during its anti-inflammatory action *in vitro*, the mRNA expression levels of PI3K, AKT and mTOR across different cell groups were measured using RT-qPCR and protein expression and phosphorylation was assessed via western blotting. Compared with the control group, the LPS group exhibited significantly increased mRNA expression of PI3K, AKT and mTOR, along with hyperactivation of phosphorylation. Treatment with varying concentrations of ORI significantly suppressed both the mRNA expression (Fig. 5A) and phosphorylation levels (Fig. 5B). No significant difference was observed between cells treated with ORI alone and the control group, demonstrating that ORI may be associated with suppressed activation of the PI3K/AKT/mTOR signaling pathway during its suppression of inflammation *in vitro*.

To further validate the effect of ORI on the PI3K/AKT/mTOR pathway *in vivo*, the phosphorylation of related proteins was examined. Compared with the control group, the DSS group showed aberrant activation of PI3K, AKT and mTOR phosphorylation. However, the DSS + 5-ASA, DSS + ORI-L and DSS + ORI-H groups showed reduced phosphorylation levels of the PI3K/AKT/mTOR pathway, with the DSS + ORI-H group exhibiting the lowest phosphorylation (Fig. 5C). In addition, the distribution and expression of p-mTOR protein in mouse colon tissues were observed, with p-mTOR being particularly aggregated at lesion sites. The DSS + 5-ASA group showed partially reduced mTOR expression, whereas the DSS + ORI-L and DSS + ORI-H groups showed more pronounced inhibition of mTOR expression (Fig. 5D). Collectively, ORI exposure was associated with reduced PI3K/AKT/mTOR pathway activation both *in vitro* and in the DSS colitis model.

Autophagy activation is associated with the anti-inflammatory patterns observed following ORI treatment. Dysregulation of autophagy has been suggested as one of the key factors contributing to the pathogenesis of UC (33). It was therefore further investigated whether ORI is associated with enhanced autophagy. The expression levels of ATG genes and proteins were assessed using western blotting and RT-qPCR. RT-qPCR analysis revealed that pretreatment with ORI increased the mRNA expression levels of ATG7, ATG5 and LC3II/I, while decreasing the mRNA level of p62. Notably, 20 μM ORI treatment resulted in a more pronounced activation of autophagy compared with the 5 μM treatment group (Fig. 6A). Western blot results demonstrated that LPS stimulation significantly reduced the expression of ATG proteins and increased p62 levels in RAW264.7 cells, suggesting that inflammatory stimulation suppressed autophagy. Treatment with ORI was

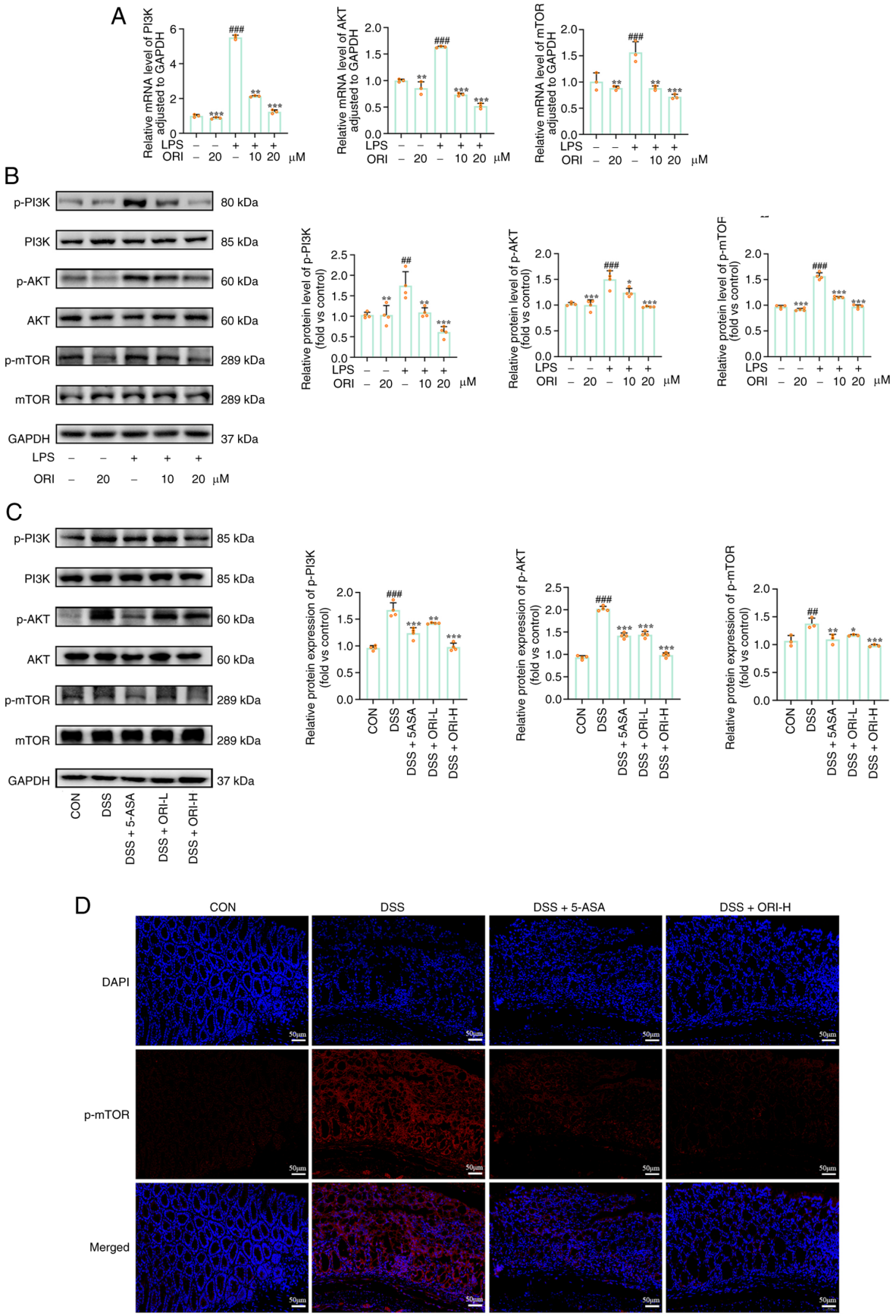

Figure 5. ORI exposure is associated with reduced activation of the PI3K/AKT/mTOR signaling pathway both *in vitro* and *in vivo*. (A) Reverse transcription-quantitative polymerase chain reaction was employed to determine the mRNA contents in cells. (B) Western blot detected the protein level in cells. (C) Western blot detected the protein level in mice. (D) Immunofluorescence for the expression of the mTOR receptor in colonic tissues. Comparison with the control group: $^{\#\#}$P<0.001, $^{\#\#\#}$P<0.0001; comparison with the DSS group: *P<0.05, **P<0.01, ***P<0.001. ORI, oridonin; LPS, lipopolysaccharide; GAPDH, glyceraldehyde-3-phosphate dehydrogenase; p-, phosphorylated; CON, control; DSS, dextran sulfate sodium; 5-ASA, 5-aminosalicylic acid; ORI-L, oridonin low-dose; ORI-H, oridonin high-dose.

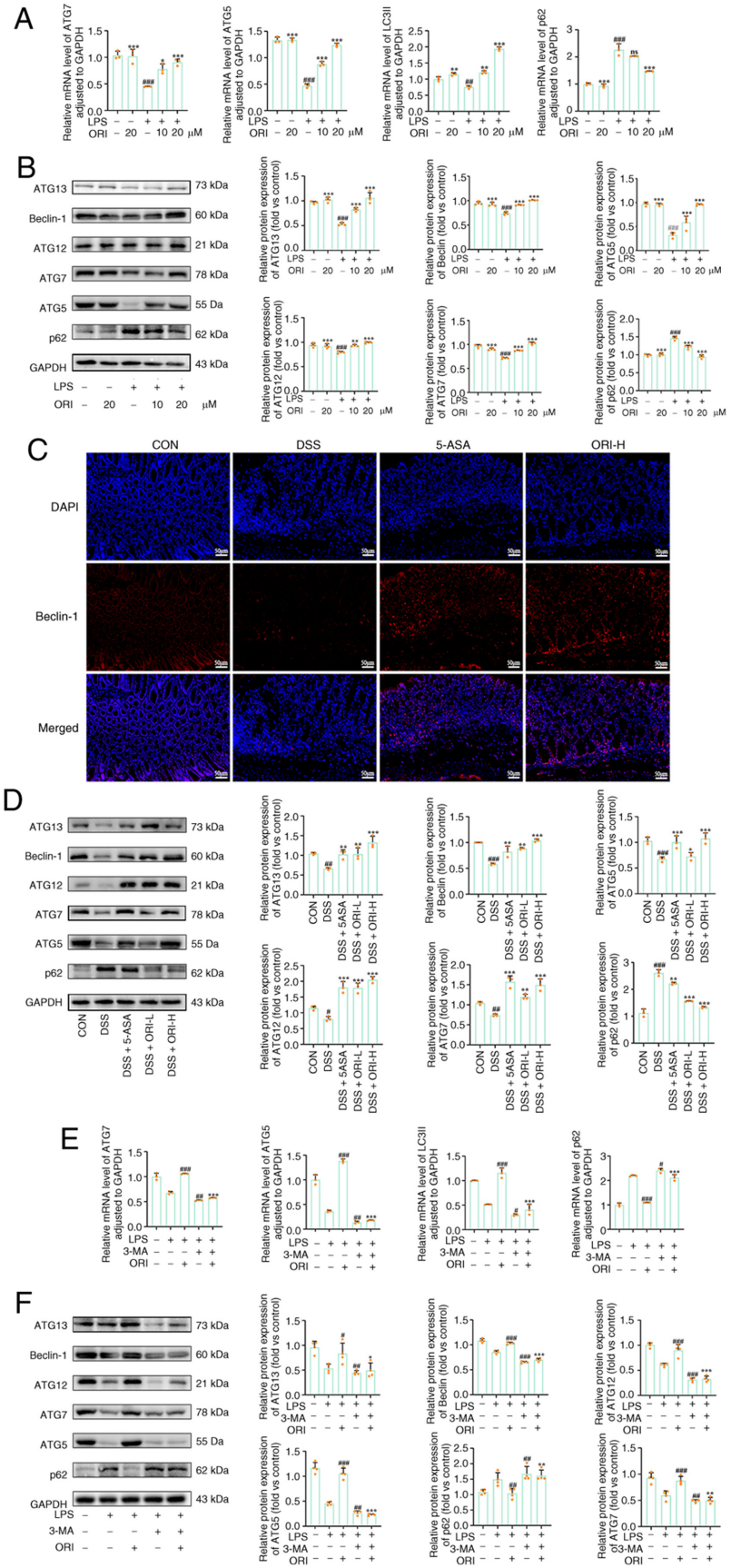

Figure 6. ORI treatment is associated with elevated autophagic signatures and 3-MA intervention weakens these autophagy-related changes. (A) RT-qPCR was employed to determine the mRNA contents in cells. (B) Western blot detected the protein level in cells. (C) Immunofluorescence for the expression of mTOR receptor in colonic tissues. (D) Western blot detected the protein level in mice. (E) RT-qPCR was employed to determine the mRNA contents in cells. (F) Western blot detected the protein level in cells. Comparison with the control group: $^{\#}$P<0.05, $^{\#\#}$P<0.01, $^{\#\#\#}$P<0.001; comparison with the DSS group: *P<0.05, **P<0.01, ***P<0.001. ns, not significant; ORI, oridonin; 3-MA, 3-methyladenine; RT-qPCR, reverse transcription-quantitative polymerase chain reaction; LPS, lipopolysaccharide; ATG, autophagy-related gene; GAPDH, glyceraldehyde-3-phosphate dehydrogenase; CON, control; DSS, dextran sulfate sodium; 5-ASA, 5-aminosalicylic acid; ORI-H, oridonin high-dose.

associated with restored autophagy activity in a dose-dependent manner, as evidenced by increased expression of ATG proteins and decreased p62 levels, indicating enhanced autophagosome formation (Fig. 6B). These findings suggested that ORI was associated with upregulated expression of ATG genes and thus enhanced autophagy in LPS-stimulated RAW264.7 cells.

To further evaluate the role of autophagy in the effects of ORI against UC, the expression of ATG proteins in colon tissues were examined using western blot and immunofluorescence staining for Beclin. DSS-induced UC led to a significant increase in p62 expression and downregulation of ATG proteins, indicating inhibition of autophagy in colon tissues. By contrast, the DSS + 5-ASA, DSS + ORI-L and DSS + ORI-H groups exhibited markedly increased expression of ATG proteins and reduced p62 levels, suggesting that drug treatments promoted autophagosome formation in the colon (Fig. 6C). Immunofluorescence staining further confirmed that ORI treatment significantly enhanced the fluorescence intensity of beclin compared with the DSS group, consistent with the western blot results (Fig. 6D). These data indicated that ORI was associated with upregulated ATG protein expression, enhanced autophagy and alleviated colon injury in DSS-induced colitis.

Furthermore, it was investigated whether the autophagy inhibitor 3-MA could attenuate the promotive effect of ORI on autophagy in LPS-stimulated RAW264.7 macrophages. RT-qPCR results showed that the LPS + 3-MA group significantly suppressed mRNA expression of ATG7, ATG5 and LC3II/I, while upregulating p62 mRNA levels (Fig. 6E). The regulatory effects of ORI on ATG7, ATG5, LC3II/I and p62 mRNA expression were markedly attenuated in the LPS + 3-MA + ORI group. Similarly, western blot analysis indicated that 3-MA treatment further inhibited the expression of ATG proteins and increased p62 levels compared with the LPS group. The promotive effect of ORI on ATG protein expression was significantly suppressed in the LPS + 3-MA + ORI group and the inhibitory effect on p62 was also weakened (Fig. 6F). These results confirmed ORI may participate in autophagy flux but cannot prove upstream causality. Notably, authentic autophagic flux was not measured via lysosomal inhibition; all autophagy-related alterations reflect indirect marker changes only.

Discussion

UC is an idiopathic, recurrent IBD characterized by abdominal pain, fatigue and hematochezia (34). A prominent pathological feature of UC is extensive inflammatory cell infiltration into the colorectal mucosa (35), with macrophages emerging as central players in orchestrating recruitment and infiltration (36). Macrophages represent one of the most prevalent leukocyte populations in the colon, and the intestine hosts the highest density of macrophages, accounting for 30-40% of intestinal leukocytes. Their phenotypic polarization can profoundly shape both innate and adaptive immune responses at the mucosal interface; when microbes breach intestinal epithelia, macrophages help preserve mucosal homeostasis via phagocytosis and cytokine secretion. Previous work has confirmed that, during inflammation, these cells release pro-inflammatory mediators such as IL-6, TNF-α and IL-1β, alongside the anti-inflammatory cytokine IL-10 (37). The present study assessed the anti-inflammatory potential of ORI *in vitro* using RAW264.7 and differentiated THP-1 cells, inducing inflammation with LPS. Notably, ORI treatment markedly lowered IL-6, TNF-α and IL-1β levels while elevating IL-10, thus providing clear evidence of its anti-inflammatory activity in cellular models. The present study focused on the critical role of macrophages in UC and confirmed that ORI can reduce the infiltration of $F4/80^+$ macrophages in colonic tissues. However, this finding alone does not confirm an anti-inflammatory macrophage phenotype, as F4/80 is a pan-macrophage marker that does not distinguish between pro-inflammatory and anti-inflammatory subsets. Previous studies have reported the potential mechanism by which ORI regulates macrophage polarization (16,38,39), and ORI-induced autophagy activation may promote the polarization of macrophages toward the M2 phenotype, thereby synergizing its anti-inflammatory effects. The present study lacks an analysis of macrophage phenotypic polarization, which prevents a comprehensive elaboration of the potential multi-level immunomodulatory effects of ORI in UC. Future studies are planned to further elucidate its therapeutic mechanisms.

Beyond the aforementioned macrophage-associated and autophagy-related changes, the therapeutic effect of ORI on UC may involve the regulation of multiple key intestinal cell types, which collectively regulate the expression of intestinal tight junction proteins and support immune homeostasis. In the context of IBD, persistent inflammatory stimuli can trigger epithelial-mesenchymal transition (EMT) in intestinal epithelial cells, ultimately driving barrier dysfunction and progressive intestinal fibrosis (40). Evidence indicates that ORI can attenuate TNF-α-induced EMT via suppressing the NF-κB pathway, thereby preserving epithelial integrity and limiting excessive fibrogenesis (41). Moreover, ORI has been reported to reduce the upregulation of endoplasmic reticulum stress-related proteins triggered by LPS, which helps sustain the survival and physiological function of intestinal epithelial cells (42). In adaptive immunity, ORI may restore the disturbed Th17/Treg balance frequently observed in UC. By inhibiting the NLRP3/IL-1β signaling axis, ORI potentially restrains excessive Th17 cell differentiation while supporting the functional recovery of regulatory T cells (38). In addition, ORI suppresses core signaling cascades including PI3K/AKT and NF-κB, both of which are critical for T-cell activation, proliferation and survival (38,43). Accumulated evidence indicates that ORI exerts inhibitory effects on Th17 cell activation and differentiation mainly via suppressing the NF-κB signaling pathway. A study has have demonstrated that ORI restrains Th1/Th17 polarization and reduces the secretion of typical Th17-related pro-inflammatory cytokines, such as IL-17 and IL-6 (44). ORI has also been reported to downregulate microglial pro-inflammatory mediators including IL-1β and IL-6, thereby remodeling the inflammatory microenvironment and indirectly affecting Th17 differentiation (44,45). In terms of immune recruitment potential, ORI can covalently target the NLRP3 inflammasome and block its assembly and activation, further limiting the release of downstream pro-inflammatory cytokines that drive the infiltration and recruitment of neutrophils and macrophages. Moreover, dual suppression of the NF-κB/NLRP3 axes may reduce the expression of chemokines, thereby restraining

the migration of Th17 cells and other immune cells toward inflamed lesions (38,46). Although the present study lacks direct experimental data on Th17 polarization, cytokine profiling and dynamic immune cell recruitment, these mechanisms deserve in-depth verification in further UC-focused investigations. Thus, these findings suggest that ORI participates in a multi-target regulatory network, acting directly on intestinal epithelial cells while indirectly modulating T lymphocytes and neutrophils. Such combined effects are conducive to reshaping adaptive immune equilibrium and upregulating tight junction protein levels in intestinal tissue. Nevertheless, most supportive evidence originates from alternative disease models or *in vitro* experimental systems; direct mechanistic validation focusing on specific cellular subsets within dedicated UC animal models or clinical samples remains limited and requires further clarification in future investigations.

At present, UC lacks targeted therapeutics in the clinic and conventional treatments achieve limited remission rates, often come with substantial costs (47). Furthermore, the high relapse rate in UC not only compromises the quality of life but also elevates colorectal cancer risk, contributing to increased mortality (48). Hence, there is a pressing demand for new pharmacologic strategies that improve immunomodulatory outcomes. In recent years, natural products sourced from herbs have shown distinctive benefits in managing chronic conditions. ORI, the primary active constituent of *Rabdosia rubescens*, displays a spectrum of pharmacological properties, including antitumor, anti-inflammatory and antibacterial effects; it has demonstrated regulatory potential in osteoarthritis and autoimmune conditions (49). Another advantage lies in its wide availability, ease of cultivation and cost-effective extraction (50). For example, ORI curbs gastric cancer cell proliferation *in vitro* and *in vivo* by downregulating vascular endothelial growth factor, integrin β3 and proliferating cell nuclear antigen (51). Meanwhile, ORI mitigates autoimmune-related cognitive impairment via PTEN/AKT pathway inhibition (52). Since UC is considered an autoimmune disorder, the present study utilized DSS to induce experimental colitis in mice (53) as this DSS-based model recapitulates key features of human UC (54). Although the ORI doses (6 and 12 mg/kg) used in the present study were determined based on preliminary experiments, no direct pharmacokinetic evidence is available to confirm that these doses achieve effective concentrations specifically in colon tissues. Existing pharmacokinetic studies have focused primarily on plasma concentrations and the reported data do not align precisely with our dosing regimen (55-58). Therefore, whether the observed therapeutic effects are mediated by local colonic accumulation of ORI or systemic actions remains to be clarified. Future studies should incorporate targeted measurements of ORI levels in colonic tissue to establish a more definitive dose-effect relationship.

To dissect the molecular mechanisms of ORI in UC, the present study adopted a network pharmacology framework (59), integrating multiple databases to identify potential overlapping targets of ORI in UC treatment. The GO/KEGG enrichment analyses further suggested a strong link between its therapeutic actions and the PI3K/AKT/mTOR signaling axis. This pathway participates broadly in cellular metabolism, growth and survival and exerts a major influence on inflammatory processes. PI3K/AKT/mTOR signaling is hyperactive in patients with UC, driving elevated cytokine secretion and symptom aggravation (60). To explore the mechanisms of ORI, RT-qPCR, western blotting and immunofluorescence analyses of RAW264.7 cells and mouse colon tissues were performed in the present study. The data revealed that ORI was associated with suppressed mRNA expression of PI3K/AKT/mTOR-related genes and curtailed phosphorylation-mediated activation. Taken together, these results support that ORI may be associated with alleviated inflammatory responses and UC pathology by restraining PI3K/AKT/mTOR activation.

Autophagy is a cellular catabolic process that degrades damaged organelles and serves as a reported downstream association of the PI3K/AKT/mTOR signaling pathway, wherein mTOR acts as a classic negative regulator of autophagy (61). Previous studies have shown that natural products can alleviate inflammatory responses by modulating autophagy. For instance, procyanidin A1 activated the AMPK/mTOR/p70S6K signaling pathway, increased the expression of beclin-1 and the LC3II/I ratio, reduced p62 levels and ameliorated colitis symptoms in colon tissues (62). In the present study, to further validate the relationship between ORI-mediated anti-inflammation and autophagy, RAW264.7 cells were treated with the autophagy inhibitor 3-MA to establish an autophagy suppression model. Notably, 3-MA treatment attenuated the anti-inflammatory effects of ORI, providing verification that autophagy activation is a core mechanism of its action. Notably, rescue experiments using PI3K/AKT/mTOR activators were not performed in the present study. Therefore, a strict causal relationship linking PI3K/AKT/mTOR inhibition directly to ORI-mediated pro-autophagic and anti-inflammatory effects cannot be concluded. The present study evaluated autophagy-associated alterations by only detecting the expression of ATG family proteins, the LC3-II/LC3-I ratio and p62 levels. Since autophagic flux assays using lysosomal inhibitors were not performed, the increased abundance of LC3-II and ATG markers cannot exclude a potential blockage during autophagosome fusion or the subsequent degradation process. Therefore, changes in autophagy described in the present study are concluded based on indirect protein markers and a productive, complete autophagic flux has not been directly demonstrated. All pathway-related interpretations are restricted to associations and definitive mechanistic validation remains necessary in follow-up investigations.

Although network pharmacology predictions and experimental data from the present study confirmed that ORI targets this pathway, the present study did not artificially reactivate the PI3K/AKT/mTOR pathway during or post-ORI treatment to determine whether its anti-inflammatory and pro-autophagic effects could be reversed. Furthermore, additional feedback mechanisms may exist within the complex regulatory network governing inflammation and autophagy. Rescue experiments could help clarify whether ORI-induced cellular or tissue responses are completely abrogated upon forced reactivation of the PI3K/AKT/mTOR pathway or if alternative compensatory protective pathways are involved, thus enabling a more in-depth elucidation of the underlying mechanism. As a chronic non-specific IBD, UC typically requires lifelong medication for patients. In subsequent studies, it is necessary to further extend the duration of ORI action to comprehensively observe the effects of long-term ORI treatment on the mouse body. Previous

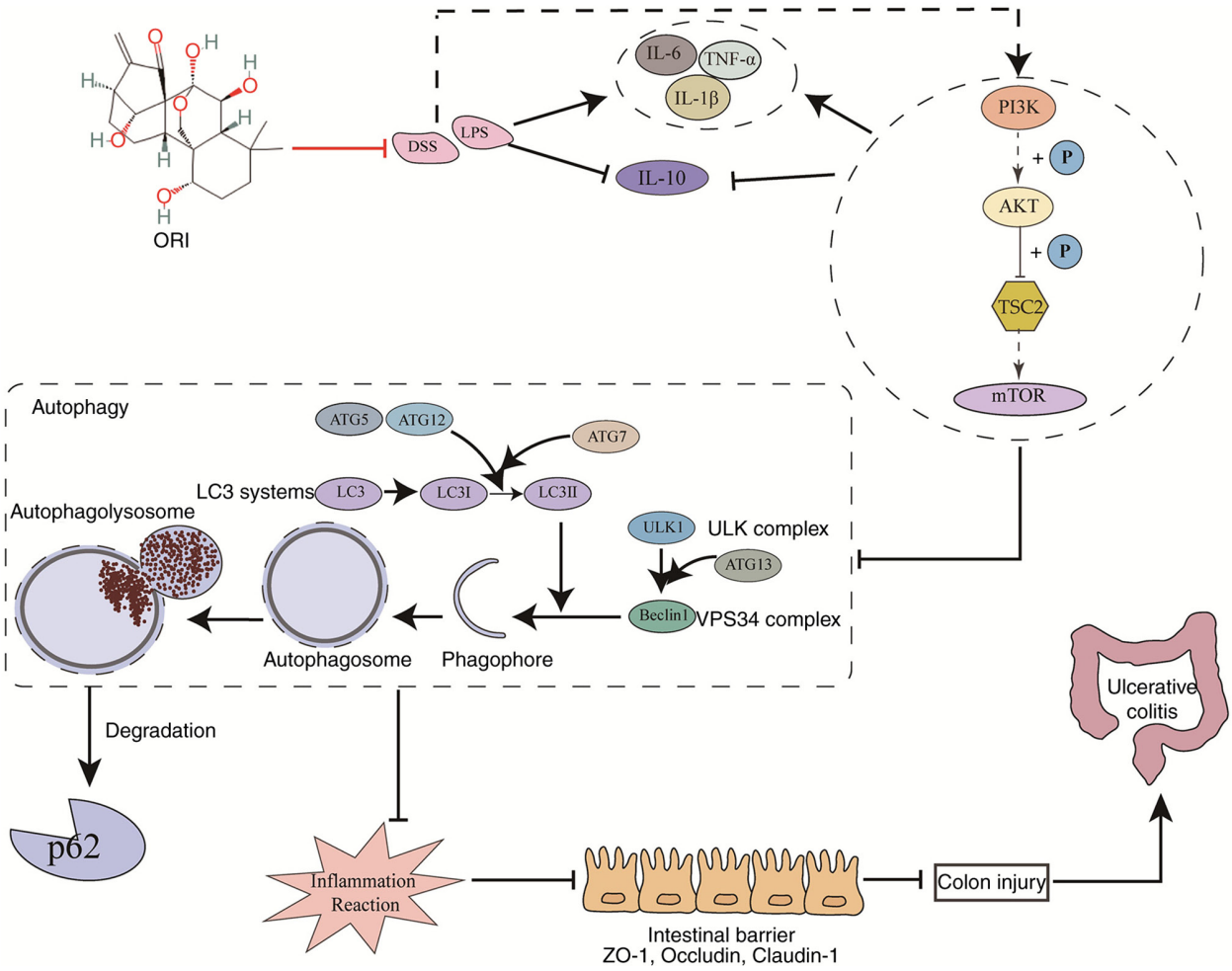

Figure 7. Schematic diagram showing the relationships observed in the present study. ORI, oridonin; DSS, dextran sulfate sodium; LPS, lipopolysaccharide; IL, interleukin; TNF, tumor necrosis factor; P, phosphorylated; TSC2, tuberous sclerosis complex 2; ZO-1, zonula occludens-1; ATG, autophagy-related gene; ULK1, unc-51 like autophagy activating kinase 1.

studies have indicated that chronic ORI administration fails to induce significant organ toxicity (63-67). Nevertheless, this evidence cannot supersede a direct safety assessment in the context of colitis models. Although the present findings offer a preliminary proof-of-concept for ORI-based UC therapy, the long-term therapeutic efficacy, optimal dosing schedule and systemic safety profile necessitate specialized examination in chronic animal models.

In colon cancer cells, ORI has been shown to induce autophagy-dependent apoptosis via the ROS/AMPK/mTOR/ULK1 signaling axis (68). This suggests that the capacity of ORI to modulate the autophagy pathway may play a pivotal role in its anti-UC effects. Rapamycin, a classic mTOR inhibitor, promotes intestinal barrier repair in UC models by inhibiting mTOR signaling and subsequently modulating the PBLD/AMOT pathway, thereby exerting immunomodulatory and tissue-protective effects through the suppression of autophagy (69). By contrast, resveratrol is a pleiotropic natural polyphenol that exerts anti-inflammatory, antioxidant and gut microbiota-modulating effects by activating multiple pathways, including AMPK and SIRT1 (70). Although it boasts a broad spectrum of action and a high safety profile, its specificity and potency are relatively limited due to its multi-target nature. Compared with rapamycin and resveratrol, ORI demonstrates unique potential in UC treatment through multi-target and multi-pathway synergistic effects. The most notable advantage of ORI lies in its ability to act as a specific covalent inhibitor of the NLRP3 inflammasome, potently blocking key inflammatory pathways at the source (38). Simultaneously, it alleviates tissue damage via the SIRT1/NF-κB/p53 pathway and promotes mucosal repair by modulating autophagy and apoptosis. These characteristics position ORI as a promising novel therapeutic candidate for UC that combines potent anti-inflammatory effects with mucosal repair capabilities. However, further in-depth research is required to fully elucidate its regulatory role in autophagy within the context of UC and to evaluate its clinical translation value.

In summary, ORI can reduce colonic injury and inflammation and suppress PI3K/AKT/mTOR activity in DSS-induced UC, alongside altering autophagy-related markers and upregulating tight junction protein expression (Fig. 7). Although ORI decreased inflammatory cytokines and macrophage infiltration, confirmation of anti-inflammatory macrophage polarization remains absent. Notably, changes in ATG proteins, LC3-II/LC3-I ratio and p62 only reflect indirect autophagy alterations; complete autophagic flux was not verified via lysosomal inhibition, so enhanced productive autophagy cannot be confirmed, and a potential fusion/degradation block cannot be

excluded. Moreover, no PI3K/AKT/mTOR rescue assays were performed, leaving the causal link between pathway suppression and ORI-mediated effects unproven. Overall, ORI shows promising therapeutic potential for UC, while key mechanistic limitations require further validation in future studies.

Acknowledgements

We thank the Dalian University Translational Medicine Research Center for providing experimental venues and instrumental equipment to support this study.

Funding

This study was supported by the National Key Research and Development Program of China (grant no. 2023YFC2508200) and the National Natural Science Foundation of China (grant no. 92369203).

Availability of data and materials

The data generated in the present study may be requested from the corresponding author.

Authors' contributions

QZ, XT and XZ designed the present study. ZM, BL, ML, NJ, HZ and YQ performed the experiments and acquired the data. ZM and BL analyzed the data. ZM and BL drafted the manuscript. ML, NJ, HZ and YQ revised the manuscript. All authors read and approved the final version of the manuscript. ZM, BL and QZ confirm the authenticity of all the raw data.

Ethics approval and consent to participate

All animal experiments were approved by the Ethics Committee of Zhongshan Hospital, Dalian University (approval no. DWLL2019060).

Patient consent for publication

Not applicable.

Competing interests

The authors declare that they have no competing interests.

Use of artificial intelligence tools

During the preparation of this work, artificial intelligence tools (DeepSeek V3.2) were used to improve the readability and language of the manuscript, and subsequently, the authors revised and edited the content produced by the artificial intelligence tools as necessary, taking full responsibility for the ultimate content of the present manuscript.

References

1. Zong Y, Meng J, Mao T, Han Q, Zhang P and Shi L: Repairing the intestinal mucosal barrier of traditional Chinese medicine for ulcerative colitis: A review. Front Pharmacol 14: 1273407, 2023.
2. Shin Y, Han S, Kwon J, Ju S, Choi T G, Kang I and Kim SS: Roles of short-chain fatty acids in inflammatory bowel disease. Nutrients 15: 4466, 2023.
3. Le Berre C, Honap S and Peyrin-Biroulet L: Ulcerative colitis. Lancet 402: 571-584, 2023.
4. Tursi A, D'Avino A, Brandimarte G, Mocci G, Pellegrino R, Savarino EV and Gravina AG; The Hericium-Uc Study Group: Enhancing oral 5-ASA effectiveness in mild-to-moderate ulcerative colitis through an H. erinaceus-based nutraceutical add-on multi-compound: The 'HERICIUM-UC' two-arm multicentre retrospective study. Pharmaceutics 16: 1133, 2024.
5. Papamichael K, Cheifetz AS, Melmed GY, Irving PM, Vande Casteele N, Kozuch PL, Raffals LE, Baidoo L, Bressler B, Devlin SM, *et al*: Appropriate therapeutic drug monitoring of biologic agents for patients with inflammatory bowel diseases. Clin Gastroenterol Hepatol 17: 1655-1668.e3, 2019.
6. Pouyan A, Ghorbanlo M, Eslami M, Jahanshahi M, Ziaei E, Salami A, Mokhtari K, Shahpasand K, Farahani N, Meybodi TE, *et al*: Glioblastoma multiforme: insights into pathogenesis, key signaling pathways, and therapeutic strategies. Mol Cancer 24: 58, 2025.
7. Lin S, Liang Y, Geng J, Yan Y, Ding R and He M: Gestational interrelationships among gut-metabolism-transcriptome in regulating early embryo implantation and placental development in mice. Microorganisms 12: 1902, 2024.
8. Huang Y, Wu Q, Li S, Lin X, Yang S, Zhu R, Fu C and Zhang Z: Harnessing nature's pharmacy: Investigating natural compounds as novel therapeutics for ulcerative colitis. Front Pharmacol 15: 1394124, 2024.
9. Chen J, Rodriguez AS, Morales MA and Fang X: Autophagy modulation and its implications on glioblastoma treatment. Curr Issues Mol Biol 45: 8687-8703, 2023.
10. Yamamoto H, Zhang S and Mizushima N: Autophagy genes in biology and disease. Nat Rev Genet 24: 382-400, 2023.
11. Zhang Z, Tan R, Xiong Z, Feng Y and Chen L: Dysregulation of autophagy during photoaging reduce oxidative stress and inflammatory damage caused by UV. Front Pharmacol 16: 1562845, 2025.
12. Pan HH, Zhou XX, Ma YY, Pan WS, Zhao F, Yu MS and Liu JQ: Resveratrol alleviates intestinal mucosal barrier dysfunction in dextran sulfate sodium-induced colitis mice by enhancing autophagy. World J Gastroenterol 26: 4945-4959, 2020.
13. Kubota M, Kakimoto K, Nakagawa T, Kobayashi E, Nakazawa K, Tawa H, Hirata Y, Okada T, Kawakami K, Asai A, *et al*: Autophagy deficiency exacerbates colitis through excessive oxidative stress and MAPK signaling pathway activation. PLoS One 14: e0225066, 2019.
14. Ren JL, Yang L, Qiu S, Zhang AH and Wang XJ: Efficacy evaluation, active ingredients, and multitarget exploration of herbal medicine. Trends Endocrinol Metab 34: 146-157, 2023.
15. Pang L, Liu H, Quan H, Sui H and Jia Y: Development of novel oridonin analogs as specifically targeted NLRP3 inflammasome inhibitors for the treatment of dextran sulfate sodium-induced colitis. Eur J Med Chem 245: 114919, 2023.
16. Han Y, Zheng Z, Chen M and Xie K: Mechanisms of macrophage polarization regulated by oridonin: A review. J Inflamm Res 18: 16545-16560, 2025.
17. Huang W, Huang M, Ouyang H, Peng J and Liang J: Oridonin inhibits vascular inflammation by blocking NF-κB and MAPK activation. Eur J Pharmacol 826: 133-139, 2018.
18. Zuo Y, Zhang CZ, Ren Q, Chen Y, Li X, Yang JR, Li HX, Tang WT, Ho HM, Sun C, *et al*: Activation of mitochondrial-associated apoptosis signaling pathway and inhibition of PI3K/Akt/mTOR signaling pathway by voacamine suppress breast cancer progression. Phytomedicine 99: 154015, 2022.
19. Zhang W, Shi L, Zhou W, Liu X, Xi Y, Wang X, Li Y, Xu X and Tang Y: Oridonin impedes breast cancer growth by blocking cells in S phase and inhibiting the PI3K/AKT/mTOR signaling pathway. Heliyon 9: e18046, 2023.
20. Ren CM, Li Y, Chen QZ, Zeng YH, Shao Y, Wu QX, Yuan SX, Yang JQ, Yu Y, Wu K, *et al*: Oridonin inhibits the proliferation of human colon cancer cells by upregulating BMP7 to activate p38 MAPK. Oncol Rep 35: 2691-2698, 2016.
21. Livak KJ and Schmittgen TD: Analysis of relative gene expression data using real-time quantitative PCR and the 2(-Delta Delta C(T)) method. Methods 25: 402-408, 2001.
22. Tang J, Diao P, Shu X, Li L and Xiong L: Quercetin and quercitrin attenuates the inflammatory response and oxidative stress in LPS-induced RAW264.7 cells: In vitro assessment and a theoretical model. Biomed Res Int 2019: 7039802, 2019.

23. Lertnimitphun P, Jiang Y, Kim N, Fu W, Zheng C, Tan H, Zhou H, Zhang X, Pei W, Lu Y and Xu H: Safranal alleviates dextran sulfate sodium-induced colitis and suppresses macrophage-mediated inflammation. Front Pharmacol 10: 1281, 2019.
24. Ellermann M, Gharaibeh RZ, Maharshak N, Pérez-Chanona E, Jobin C, Carroll IM, Arthur JC, Plevy SE, Fodor AA, Brouwer CR and Sartor RB: Dietary iron variably modulates assembly of the intestinal microbiota in colitis-resistant and colitis-susceptible mice. Gut Microbes 11: 32-50, 2020.
25. Motomura Y, Khan WI, El-Sharkawy RT, Verma-Gandhu M, Verdu EF, Gauldie J and Collins SM: Induction of a fibrogenic response in mouse colon by overexpression of monocyte chemoattractant protein 1. Gut 55: 662-670, 2006.
26. Digby-Bell JL, Atreya R, Monteleone G and Powell N: Interrogating host immunity to predict treatment response in inflammatory bowel disease. Nat Rev Gastroenterol Hepatol 17: 9-20, 2020.
27. Wu MY, Liu L, Wang EJ, Xiao HT, Cai CZ, Wang J, Su H, Wang Y, Tan J, Zhang Z, *et al*: PI3KC3 complex subunit NRBF2 is required for apoptotic cell clearance to restrict intestinal inflammation. Autophagy 17: 1096-1111, 2021.
28. Mao X, Li W, Chen W, Li Y, Wang Q, Wang X, Pi Z, Wang D, Xu H, Guo Q, *et al*: Exploring and characterizing a novel combination of paeoniflorin and talatizidine for the treatment of rheumatoid arthritis. Pharmacol Res 153: 104658, 2020.
29. Ma JX, Wang B, Li HS, Yu J, Hu HM, Ding CF and Chen WQ: Uncovering the mechanisms of leech and centipede granules in the treatment of diabetes mellitus-induced erectile dysfunction utilising network pharmacology. J Ethnopharmacol 265: 113358, 2021.
30. Li Y, Bai W and Zhang L: The overexpression of CD80 and ISG15 are associated with the progression and metastasis of breast cancer by a meta-analysis integrating three microarray datasets. Pathol Oncol Res 26: 443-452, 2020.
31. Zhang C, Li H, Yuan C, Liu S, Li M, Zhu J, Lin X, Lu Y and Guo X: CKB1 regulates expression of ribosomal protein L10 family gene and plays a role in UV-B response. Plant Biol (Stuttg) 22 (Suppl 1): S143-S152, 2020.
32. Xu Y, Tan M, Ma X, Li H, He X, Chen Z, Tan Y, Nie W, Rong P and Wang W: Human mesenchymal stem cells-derived conditioned medium inhibits hypoxia-induced death of neonatal porcine islets by inducing autophagy. Xenotransplantation 27: e12556, 2020.
33. Xu Y, Shen J and Ran Z: Emerging views of mitophagy in immunity and autoimmune diseases. Autophagy 16: 3-17, 2020.
34. Wu B, Tong J and Ran Z: Tacrolimus therapy in steroid-refractory ulcerative colitis: A review. Inflamm Bowel Dis 26: 24-32, 2020.
35. Qiu S, Li P, Zhao H and Li X: Maresin 1 alleviates dextran sulfate sodium-induced ulcerative colitis by regulating NRF2 and TLR4/NF-kB signaling pathway. Int Immunopharmacol 78: 106018, 2020.
36. Cossu G, Kuo AL, Pessano S, Warren L and Cooper RA: Decreased synthesis of high-molecular-weight glycopeptides in human promyelocytic leukemic cells (HL-60) during phorbol ester-induced macrophage differentiation. Cancer Res 42: 484-489, 1982.
37. Shahidullah A, Lee JY, Kim YJ, Halimi SMA, Rauf A, Kim HJ, Kim BY and Park W: Anti-inflammatory effects of diospyrin on lipopolysaccharide-induced inflammation using RAW 264.7 mouse macrophages. Biomedicines 8: 11, 2020.
38. He H, Jiang H, Chen Y, Ye J, Wang A, Wang C, Liu Q, Liang G, Deng X, Jiang W and Zhou R: Oridonin is a covalent NLRP3 inhibitor with strong anti-inflammasome activity. Nat Commun 9: 2550, 2018.
39. Ikezoe T, Yang Y, Bandobashi K, Saito T, Takemoto S, Machida H, Togitani K, Koeffler HP and Taguchi H: Oridonin, a diterpenoid purified from *Rabdosia rubescens*, inhibits the proliferation of cells from lymphoid malignancies in association with blockade of the NF-kappa B signal pathways. Mol Cancer Ther 4: 578-586, 2005.
40. Macias-Ceja DC, Mendoza-Ballesteros MT, Ortega-Albiach M, Barrachina MD and Ortiz-Masià D: Role of the epithelial barrier in intestinal fibrosis associated with inflammatory bowel disease: Relevance of the epithelial-to mesenchymal transition. Front Cell Dev Biol 11: 1258843, 2023.
41. Wang X, Cummins C, Gu Y, Song J, Zhou J and Radhakrishnan R: Therapeutic effect of oridonin against inflammatory bowel disease involves inhibition of intestinal fibrosis via NF-κB pathway. FASEB J 34: 1, 2020.
42. Jiang J, Zhang N, Song H, Yang Y, Li J and Hu X: Oridonin alleviates the inhibitory effect of lipopolysaccharide on the proliferation and osteogenic potential of periodontal ligament stem cells by inhibiting endoplasmic reticulum stress and NF-κB/NLRP3 inflammasome signaling. BMC Oral Health 23: 137, 2023.
43. Song M, Liu X, Liu K, Zhao R, Huang H, Shi Y, Zhang M, Zhou S, Xie H, Chen H, *et al*: Targeting AKT with oridonin inhibits growth of esophageal squamous cell carcinoma in vitro and patient-derived xenografts in vivo. Mol Cancer Ther 17: 1540-1553, 2018.
44. Wang S, Zhang Y, Saas P, Wang H, Xu Y, Chen K, Zhong J, Yuan Y, Wang Y and Sun Y: Oridonin's therapeutic effect: Suppressing Th1/Th17 simultaneously in a mouse model of Crohn's disease. J Gastroenterol Hepatol 30: 504-512, 2015.
45. Wang S, Yang H, Yu L, Jin J, Qian L, Zhao H, Xu Y and Zhu X: Oridonin attenuates Aβ1-42-induced neuroinflammation and inhibits NF-κB pathway. PLoS One 9: e104745, 2014.
46. Du X, Que W, Hu X, Yu X, Guo WZ, Zhang S and Li XK: Oridonin prolongs the survival of mouse cardiac allografts by attenuating the NF-κB/NLRP3 pathway. Front Immunol 12: 719574, 2021.
47. Van de Meeberg MM, Schultheiss JPD, Oldenburg B, Fidder HH and Huitema ADR: Does the 5-aminosalicylate concentration correlate with the efficacy of oral 5-aminosalicylate and predict response in patients with inflammatory bowel disease? A systematic review. Digestion 101: 245-261, 2020.
48. Dong C, Metzger M, Holsbø E, Perduca V and Carbonnel F: Systematic review with meta-analysis: Mortality in acute severe ulcerative colitis. Aliment Pharmacol Ther 51: 8-33, 2020.
49. Sarwar MS, Xia YX, Liang ZM, Tsang SW and Zhang HJ: Mechanistic pathways and molecular targets of plant-derived anticancer ent-kaurane diterpenes. Biomolecules 10: 144, 2020.
50. Zhang Y, Wang S, Dai M, Nai J, Zhu L and Sheng H: Solubility and bioavailability enhancement of oridonin: A review. Molecules 25: 332, 2020.
51. Yang Q, Ma W, Yu K, Zhang Q, Ye Z, Xia W and Li S: Oridonin suppresses human gastric cancer growth in vitro and in vivo via inhibition of VEGF, integrin β3, and PCNA. Biol Pharm Bull 43: 1035-1045, 2020.
52. Wen F, Zhuge W, Wang J, Lu X, You R, Liu L, Zhuge Q and Ding S: Oridonin prevents insulin resistance-mediated cognitive disorder through PTEN/Akt pathway and autophagy in minimal hepatic encephalopathy. J Cell Mol Med 24: 61-78, 2020.
53. Cooper HS, Murthy SN, Shah RS and Sedergran DJ: Clinicopathologic study of dextran sulfate sodium experimental murine colitis. Lab Invest 69: 238-249, 1993.
54. Min X, Guo Y, Zhou Y and Chen X: Protection against dextran sulfate sodium-induced ulcerative colitis in mice by neferine, a natural product from Nelumbo nucifera Gaertn. Cell J 22: 523-531, 2021.
55. Wang M, Xu B, Liu L and Wang D: Oridonin attenuates dextran sulfate sodium-induced ulcerative colitis in mice via the Sirt1/NF-κB/p53 pathway. Mol Med Rep 26: 312, 2022.
56. Zou BH, Tan YH, Deng WD, Zheng JH, Yang Q, Ke MH, Ding ZB and Li XJ: Oridonin ameliorates inflammation-induced bone loss in mice via suppressing DC-STAMP expression. Acta Pharmacol Sin 42: 744-754, 2021.
57. Yan C, Yan H, Mao J, Liu Y, Xu L, Zhao H, Shen J, Cao Y, Gao Y, Li K and Jin W: Neuroprotective effect of oridonin on traumatic brain injury via inhibiting NLRP3 inflammasome in experimental mice. Front Neurosci 14: 557170, 2020.
58. Li X, Zhang CT, Ma W, Xie X and Huang Q: Oridonin: A review of its pharmacology, pharmacokinetics and toxicity. Front Pharmacol 12: 645824, 2021.
59. Wang X, Wang ZY, Zheng JH and Li S: TCM network pharmacology: A new trend towards combining computational, experimental and clinical approaches. Chin J Nat Med 19: 1-11, 2021.
60. Huang XL, Xu J, Zhang XH, Qiu BY, Peng L, Zhang M and Gan HT: PI3K/Akt signaling pathway is involved in the pathogenesis of ulcerative colitis. Inflamm Res 60: 727-734, 2011.
61. Sun L, Zheng W, Liu QD and Ge L: Valproic acid protects chondrocytes from LPS-stimulated damage via regulating miR-302d-3p/ITGB4 axis and mediating the PI3K-AKT signaling pathway. Front Mol Biosci 8: 633315, 2021.
62. Zhang H, Lang W, Liu X, Bai J, Jia Q and Shi Q: Procyanidin A1 alleviates DSS-induced ulcerative colitis via regulating AMPK/mTOR/p70S6K-mediated autophagy. J Physiol Biochem 78: 213-227, 2022.

63. Zhou F, Gao H, Shang L, Li J, Zhang M, Wang S, Li R, Ye L and Yang S: Oridonin promotes endoplasmic reticulum stress via TP53-repressed TCF4 transactivation in colorectal cancer. J Exp Clin Cancer Res 42: 150, 2023.
64. Zhou GB, Kang H, Wang L, Gao L, Liu P, Xie J, Zhang FX, Weng XQ, Shen ZX, Chen J, *et al*: Oridonin, a diterpenoid extracted from medicinal herbs, targets AML1-ETO fusion protein and shows potent antitumor activity with low adverse effects on t(8;21) leukemia in vitro and in vivo. Blood 109: 3441-3450, 2007.
65. Liu Y, Wang X, Feng H, Li X, Yang R, Zhang M, Du Y, Liu R, Luo M, Li Z, *et al*: Glutathione-depleting liposome adjuvant for augmenting the efficacy of a glutathione covalent inhibitor oridonin for acute myeloid leukemia therapy. J Nanobiotechnology 22: 299, 2024.
66. Chen Y, Jiang H, Zhan Z, Lu J, Gu T, Yu P, Liang W, Zhang X, Zhong S and Tang L: Oridonin restores hepatic lipid homeostasis in an LXRα-ATGL/EPT1 axis-dependent manner. J Pharm Anal 13: 1281-1295, 2023.
67. Zhong B, Peng W, Du S, Chen B, Feng Y, Hu X, Lai Q, Liu S, Zhou ZW, Fang P, *et al*: Oridonin inhibits SARS-CoV-2 by targeting Its 3C-like protease. Small Sci 2: 2100124, 2022.
68. Shao B, Bu H, Li G, Kang D and Ju Q: Autophagy-dependent apoptosis induction by oridonin are mediated by ROS-dependent AMPK-mTOR-ULK1 pathway in colon cancer. Am J Cancer Res 15: 1902-1918, 2025.
69. Tang X, Huang Y, Zhu Y and Xu Y: Immune dysregulation in ulcerative colitis: Pathogenic mechanisms and therapeutic strategies of traditional Chinese medicine. Front Cell Dev Biol 13: 1610435, 2025.
70. Ding Y, Ding C, Ye N, Liu Z, Wold EA, Chen H, Wild C, Shen Q and Zhou J: Discovery and development of natural product oridonin-inspired anticancer agents. Eur J Med Chem 122: 102-117, 2016.